

Copula-Based Aggregation and Context-Aware Conformal Prediction for Reliable Renewable Energy Forecasting

Alireza Moradi, Mathieu Tanneau, Reza Zandehshahvar, Pascal Van Hentenryck

NSF Artificial Intelligence Institute for Advances in Optimization

H. Milton Stewart School of Industrial and Systems Engineering

Georgia Institute of Technology, Atlanta, GA, USA

alirezamoradi@gatech.edu, {mathieu.tanneau, reza, pascal.vanhentenryck}@isye.gatech.edu

Abstract—The rapid growth of renewable energy penetration has intensified the need for reliable probabilistic forecasts to support grid operations at aggregated (fleet or system) levels. In practice, however, system operators often lack access to fleet-level probabilistic models and instead rely on site-level forecasts produced by heterogeneous third-party providers. Constructing coherent and calibrated fleet-level probabilistic forecasts from such inputs remains challenging due to complex cross-site dependencies and aggregation-induced miscalibration. This paper proposes a calibrated probabilistic aggregation framework that directly converts site-level probabilistic forecasts into reliable fleet-level forecasts in settings where system-level models cannot be trained or maintained. The framework integrates copula-based dependence modeling to capture cross-site correlations with Context-Aware Conformal Prediction (CACP) to correct miscalibration at the aggregated level. This combination enables dependence-aware aggregation while providing valid coverage and maintaining sharp prediction intervals. Experiments on large-scale solar generation datasets from MISO, ERCOT, and SPP demonstrate that the proposed Copula+CACP approach consistently achieves near-nominal coverage with significantly sharper intervals than uncalibrated aggregation baselines.

Index Terms—Renewable Energy, Copula Aggregation, Conformal Prediction, Probabilistic Forecasting

I. INTRODUCTION

A. Motivation and Related Works

As the penetration of renewable energy sources, particularly wind and solar, continues to increase in modern power systems, operational and planning uncertainty has grown substantially. This transition toward weather-dependent generation introduces significant variability, making deterministic forecasts insufficient for reliable grid operation. As a result, probabilistic forecasting has become a critical component of decision-making in power systems by providing uncertainty-aware estimates of generation, demand, and other key system variables [1].

Motivated by this need, considerable advances have been made in probabilistic renewable energy forecasting. Existing methods span a broad methodological spectrum, ranging from classical statistical approaches such as ARIMA [2], to machine learning techniques including Random Forests [3] and Support Vector Machines [4], and more recently to deep learning architectures such as recurrent neural networks (RNNs) [5] and other advanced neural forecasting models [6]. Comprehensive reviews of probabilistic forecasting methods for renewable energy can be found in [7]–[12].

Despite these advances, constructing accurate probabilistic forecasts at high aggregation levels, such as regional

zones or system-wide renewable fleets, remains a significant challenge. Reliable fleet-level forecasting typically requires high-resolution meteorological inputs, site-specific operational characteristics, and continuously updated configuration information across a large number of assets. Collecting, maintaining, and synchronizing such data at scale is often costly and operationally demanding. Furthermore, aggregated renewable generation exhibits complex spatio-temporal dependencies arising from heterogeneous site behaviors and large-scale weather dynamics, which are difficult to capture using a single centralized forecasting model [13], [14].

Consequently, in many practical settings, probabilistic forecasts are available at lower hierarchical levels (e.g., individual sites or sub-regions) but not at higher aggregation levels (e.g., fleet or system level), despite their critical importance for grid operation and optimization. This has led to growing interest in probabilistic forecast aggregation within hierarchical renewable energy systems. Existing approaches include copula-based bottom-up frameworks that construct coherent system-level distributions from site-level forecasts [15], [16], clustering-based copula aggregation methods designed to reduce computational complexity [17], and copula models that explicitly learn cross-site dependence structures for fleet-level forecasting [18]–[20]. However, the aggregated forecasts produced by these methods are often miscalibrated, primarily due to imperfect dependence modeling, structural errors in site-level probabilistic forecasts, and model misspecification.

Conformal prediction (CP) provides a principled approach to addressing the miscalibration of probabilistic forecasts, offering distribution-free coverage guarantees under mild assumptions while maintaining relatively low computational complexity [21]. Its adoption in renewable energy forecasting has grown rapidly, particularly for uncertainty quantification in solar and wind power generation. For instance, [6] combines split conformal prediction with quantile random forests for wind power forecasting, while [22] proposes an asymmetric multi-quantile conformal adjustment strategy to improve day-ahead wind prediction intervals. In solar generation forecasting, [23] evaluates weighted, KNN-based, and Mondrian CP variants for constructing calibrated intervals. More recently, [24] introduces context-aware conformal prediction (CACP), which incorporates contextual weighting to produce efficient (i.e., sharper) prediction intervals tailored to renewable energy applications.

Motivated by an operational need identified through collaboration with an industry partner, this paper proposes a

calibrated probabilistic aggregation framework for scenarios in which only lower-level probabilistic forecasts are available and fleet-level models cannot be directly trained. In the proposed approach, site-level probabilistic forecasts are first aggregated using a copula-based dependence model to construct a coherent fleet-level predictive distribution followed by a calibration step using CP. The proposed method ensures valid coverage while preserving interval sharpness for fleet-level probabilistic forecasts. Overall, the proposed method delivers reliable fleet-level probabilistic forecasts without retraining site-level models or requiring access to proprietary site-level data, making it well suited for practical hierarchical forecasting settings.

B. Contributions and Outline

This paper makes the following key contributions:

- Proposes a calibrated aggregation framework that takes probabilistic forecasts from arbitrary site-level forecasting models as input and produces reliable and sharp fleet-level probabilistic forecasts by combining copula-based aggregation with context-aware conformal prediction (CACP).
- Addresses a practical industry challenge in renewable energy forecasting, where reliable fleet- or system-level probabilistic forecasts are often unavailable despite the availability of forecasts at individual site or zone levels.
- Demonstrates the effectiveness of the proposed method through extensive experiments on large U.S. power systems, including MISO, SPP, and ERCOT, demonstrating substantial improvements over existing baselines such as Copula-only aggregation and NREL system-level forecasts.

The proposed method is compared against several baselines, including NREL system-level forecasts, uncalibrated copula aggregation, and conformal calibration approaches applied at both the system and aggregated levels. Results show that the proposed method, Copula+CACP, consistently achieves near-target coverage with sharper prediction intervals than all competing baselines.

II. PROBLEM FORMULATION

This section formalizes the probabilistic aggregation setting considered in this work. Marginal probabilistic forecasts are assumed to be available at the individual site level. The objective is to construct a reliable fleet-level probabilistic forecast that (i) coherently accounts for cross-site dependence structures and (ii) achieves calibrated uncertainty coverage at the aggregated level.

A. Problem Setting

Consider a system comprising $\mathcal{N} = \{1, \dots, N\}$ renewable generation sites (e.g., solar plants) observed over historical time indices $\mathcal{T} = \{1, \dots, T\}$. Let $x_{i,t}$ denote the realized power output of site $i \in \mathcal{N}$ at time $t \in \mathcal{T}$, and define the matrix of all observations as:

$$\mathbf{X}_{\cdot, \tau} = \begin{bmatrix} | & \dots & | \\ \mathbf{x}_{\cdot, 1} & \dots & \mathbf{x}_{\cdot, T} \\ | & \dots & | \end{bmatrix} \in \mathbb{R}^{N \times T}, \quad (1)$$

where $\mathbf{x}_{\cdot, t} = [x_{1,t}, \dots, x_{N,t}]$. For each site $i \in \mathcal{N}$ and time $t \in \mathcal{T}$, a probabilistic forecasting model provides a marginal predictive cumulative distribution function (CDF) $\hat{F}_{i,t}$. Without loss of generality, these marginal predictive distributions are assumed to be available in quantile form. The marginal forecasts are univariate and do not encode explicit spatial dependencies across sites, which commonly occurs when site-level forecasts are generated independently or obtained from heterogeneous forecasting providers.

The aggregated (fleet-level) power generation is defined as:

$$x_{0,t} = \sum_{i=1}^N x_{i,t}, \quad t \in \mathcal{T}. \quad (2)$$

Given a future time index $\tau > T$ and site-level marginal forecasts $\{\hat{F}_{i,\tau}\}_{i \in \mathcal{N}}$, the objective is to construct a calibrated prediction interval for the aggregated output at a pre-specified confidence level $1 - \alpha$ with $\alpha \in (0, 1)$. Specifically, the goal is to produce an interval

$$\tilde{C}_{0,\tau}^\alpha = [\tilde{q}_{0,\tau}^{\alpha/2}, \tilde{q}_{0,\tau}^{1-\alpha/2}], \quad (3)$$

such that it satisfies the marginal coverage guarantee

$$\mathbb{P}(x_{0,\tau} \in \tilde{C}_{0,\tau}^\alpha) \geq 1 - \alpha. \quad (4)$$

Constructing $\tilde{C}_{0,\tau}^\alpha$ is challenging for two main reasons. First, cross-site dependencies must be accurately captured when aggregating marginal forecasts, as ignoring spatial correlations can lead to biased or overly narrow uncertainty estimates at the fleet level. Second, even when site-level probabilistic forecasts are well specified, prediction intervals derived from the aggregated distribution may be miscalibrated due to error propagation and model mismatch introduced during aggregation.

To address these challenges, Section III outlines the proposed framework for constructing calibrated and sharp fleet-level prediction intervals, combining copula-based aggregation with conformal calibration techniques.

III. METHODOLOGY

The proposed framework consists of two main stages. First, site-level probabilistic forecasts are aggregated into a fleet-level predictive distribution using a Gaussian copula, which captures cross-site dependencies and enables probabilistic aggregation via Monte Carlo sampling. The resulting aggregated forecasts are then calibrated using CACP.

A. Aggregation Stage

Copula functions provide a principled framework for constructing multivariate distributions by separating marginal behavior from the dependence structure. This property makes copulas particularly well-suited for probabilistic aggregation, where marginal forecasts are available but cross-variable

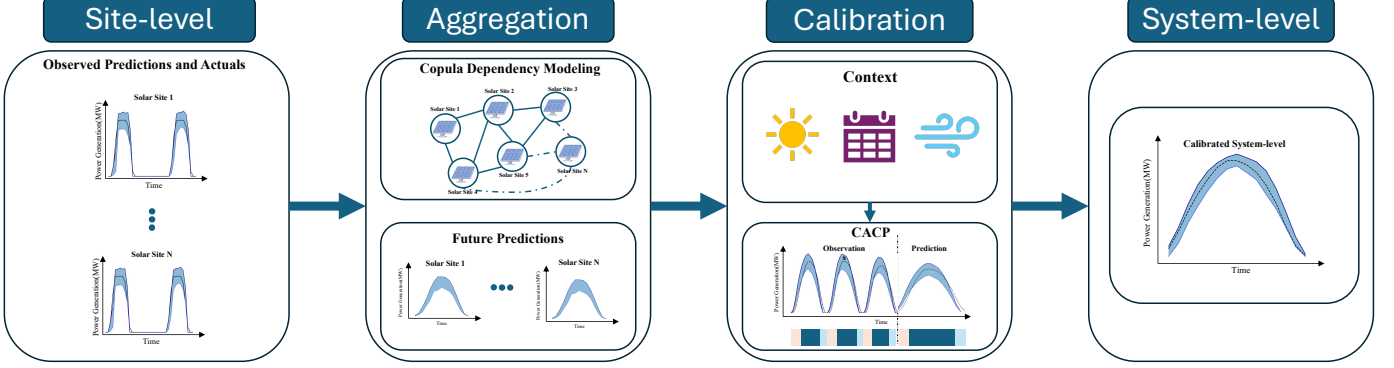


Fig. 1. Conceptual overview of the proposed probabilistic aggregation framework. Site-level marginal forecasts are first combined using copula-based dependency modeling to construct an aggregated predictive distribution. A context-aware conformal calibration step (CACP) is then applied to obtain calibrated and sharp fleet-level probabilistic forecasts.

dependencies must be modeled explicitly. Formally, a copula is defined as follows:

Definition 1 (Copula). *Let $d \in \mathbb{Z}_+$. A function $\mathbf{C} : [0, 1]^d \rightarrow [0, 1]$ is a copula if it is the cumulative distribution function (CDF) of a d -dimensional random variable whose marginal distributions are all uniform on $[0, 1]$.*

The fundamental connection between joint and marginal distributions is given by Sklar's theorem, which underpins copula-based aggregation.

Theorem 1 (Sklar's Theorem [25]). *Let \mathbf{Y} be a d -dimensional random variable with joint CDF \mathbf{F} and marginal CDFs $\{F_i\}_{i=1}^d$. There exists a copula function $\mathbf{C} : [0, 1]^d \rightarrow [0, 1]$ such that*

$$\mathbf{F}(y_1, \dots, y_d) = \mathbf{C}(F_1(y_1), \dots, F_d(y_d)). \quad (5)$$

Sklar's theorem enables modeling the joint distribution of site-level generation by combining marginal predictive distributions with a copula that captures cross-site dependencies.

Following the notation introduced in Section II, historical observations $\{x_{i,t}\}$ and their corresponding site-level marginal predictive CDFs $\{\hat{F}_{i,t}\}$ are considered. To capture cross-site dependencies, the probability integral transform is applied to each marginal forecast,

$$\hat{y}_{i,t} = \hat{F}_{i,t}(x_{i,t}), \quad (6)$$

where $\hat{y}_{i,t} \in [0, 1]$ under calibrated marginals. Let Φ denote the standard normal CDF and define

$$\hat{z}_{i,t} = \Phi^{-1}(\hat{y}_{i,t}), \quad (7)$$

which are stacked into the matrix $\hat{\mathbf{Z}} \in \mathbb{R}^{N \times T}$. The empirical correlation matrix

$$\hat{\Sigma} = \frac{1}{T} \hat{\mathbf{Z}} \hat{\mathbf{Z}}^\top \quad (8)$$

serves as the correlation parameter of a Gaussian copula $\mathbf{C}_{\hat{\Sigma}}$, encoding cross-site dependencies. Note that the correlation matrix is estimated using only the historical data.

Given a future time $\tau > T$ with available site-level marginal forecasts $\{\hat{F}_{i,\tau}\}_{i \in \mathcal{N}}$, the joint predictive distribution of site-level generation is represented as:

$$\hat{\mathbf{F}}_\tau(x_{1,\tau}, \dots, x_{N,\tau}) = \mathbf{C}_{\hat{\Sigma}}(\hat{F}_{1,\tau}(x_{1,\tau}), \dots, \hat{F}_{N,\tau}(x_{N,\tau})). \quad (9)$$

As closed-form aggregation is generally infeasible, Monte Carlo sampling is used to approximate the aggregated distribution. Samples are drawn from a multivariate normal distribution,

$$\tilde{\mathbf{Z}} \sim \mathcal{MVN}(0, \hat{\Sigma}), \quad (10)$$

transformed via Φ to uniforms, and mapped through the marginal inverse CDFs, given a set of S samples:

$$\tilde{x}_{i,\tau}^{(s)} = \hat{F}_{i,\tau}^{-1}(\tilde{y}_{i,\tau}^{(s)}), \quad s = 1, \dots, S. \quad (11)$$

Fleet-level generation samples are obtained as follows:

$$\tilde{x}_{0,\tau}^{(s)} = \sum_{i=1}^N \tilde{x}_{i,\tau}^{(s)}, \quad (12)$$

yielding an empirical approximation of the aggregated predictive distribution $\hat{F}_{0,\tau}$.

B. Calibration Stage

Although copula-based aggregation captures cross-site dependencies, prediction intervals derived from the aggregated distribution may fail to satisfy the marginal coverage guarantee in (4). This motivates a post-hoc calibration step at the aggregated level.

a) *Conformalized Quantile Regression (CQR)*: This approach provides a distribution-free mechanism for calibrating predictive intervals by combining quantile regression with CP, yielding finite-sample marginal coverage guarantees while adapting to heteroscedastic forecast errors [26].

Given a miscoverage level $\alpha \in [0, 1]$, CQR starts from a given prediction interval $\hat{C}_t^\alpha(x_t) = [\hat{q}^{\alpha/2}, \hat{q}^{1-\alpha/2}]$. Calibration is performed on a held-out calibration set \mathcal{T}_{cal} by defining, for each $\tau \in \mathcal{T}_{cal}$, the conformity score

$$s_\tau = \max(\hat{q}^{\alpha/2}(x_\tau) - y_\tau, y_\tau - \hat{q}^{1-\alpha/2}(x_\tau)), \quad (13)$$

which measures the deviation of the observed outcome from the predicted interval. The conformalized prediction interval is then obtained as

$$\tilde{C}_t^\alpha(x_t) = [\hat{q}^{\alpha/2}(x_t) - \hat{s}, \hat{q}^{1-\alpha/2}(x_t) + \hat{s}], \quad (14)$$

where

$$\hat{s} = Q^{1-\alpha}(\{s_\tau\}_{\tau \in \mathcal{T}_{cal}}). \quad (15)$$

Under the exchangeability assumption, the resulting interval satisfies the desired marginal coverage guarantee [26].

b) *Weighted Conformal Prediction*.: Standard CQR assigns equal importance to all calibration samples, implicitly assuming global exchangeability between calibration and test points. In renewable energy forecasting, forecast errors are strongly regime-dependent, which may lead to conservative or locally miscalibrated intervals. To address this limitation, weighted conformal prediction is adopted.

Let t denote a test instance with context vector c_t . Each calibration sample $\tau \in \mathcal{T}_{cal}$ is assigned a non-negative similarity weight

$$w_\tau = \psi(c_t, c_\tau), \quad w_\tau \geq 0, \quad (16)$$

where $\psi(\cdot, \cdot)$ is a similarity function. The weights are normalized as

$$p_\tau = \frac{w_\tau}{\sum_{\tau' \in \mathcal{T}_{cal}} w_{\tau'}}. \quad (17)$$

Instead of using an unweighted empirical quantile of conformity scores, the conformal correction is computed using a weighted quantile:

$$\hat{s} = Q^{1-\alpha}(\{(s_\tau, p_\tau)\}_{\tau \in \mathcal{T}_{cal}}), \quad (18)$$

leading to the calibrated prediction interval

$$\tilde{C}_t^\alpha = [\hat{q}_t^{\alpha/2} - \hat{s}, \hat{q}_t^{1-\alpha/2} + \hat{s}]. \quad (19)$$

When the weights are uniform, the procedure reduces to standard CQR. Under weighted exchangeability assumptions, valid marginal coverage guarantees are retained [27].

c) *Context-Aware Conformal Prediction (CACP)*: Building on weighted CP, CACP implements a context-aware calibration strategy by defining similarity weights using physically meaningful auxiliary features, enabling calibration to adapt to local operating regimes while preserving statistical validity. In this work, similarity is defined using a radial basis function (RBF) kernel:

$$\psi(c_t, c_\tau) = \exp(-\gamma \|c_t - c_\tau\|^2), \quad (20)$$

where $\gamma > 0$ controls the degree of localization of the weighting. This kernel-based similarity emphasizes calibration samples that are most relevant to the test instance. Although the framework allows alternative non-negative similarity functions, the RBF kernel is used throughout this study.

The context vector c_t is constructed from physically meaningful auxiliary features designed to capture temporal structure and operating regimes in solar generation. Specifically, it includes lagged historical generation values ($H_{t,k}^l$), periodic time embeddings ($\xi_t^h, \xi_t^d, \xi_t^m$), and a normalized representation of the solar day (ξ_t^s). Formally,

$$c_t = (H_{t,k}^l, \xi_t^h, \xi_t^d, \xi_t^m, \xi_t^s). \quad (21)$$

These features allow CACP to adapt prediction intervals to local operating conditions while maintaining statistical validity.

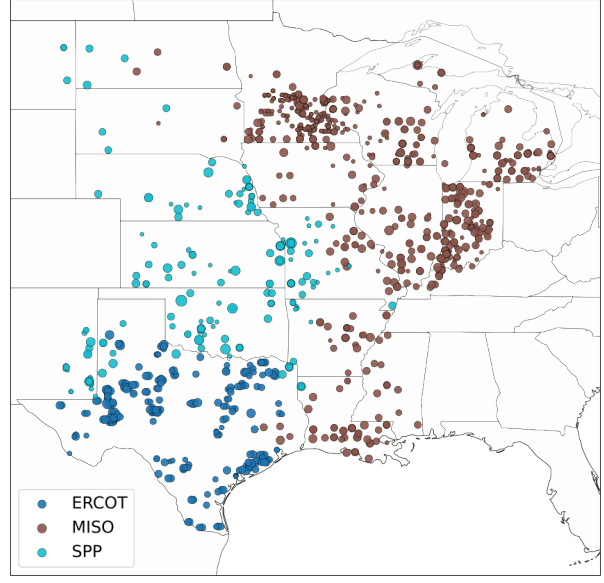


Fig. 2. Spatial distribution of solar generation sites across MISO, ERCOT, and SPP, illustrating the geographic diversity of the systems evaluated in this work.

IV. EXPERIMENTAL SETTING

A. Data

The experiments are performed on large-scale datasets from key U.S. power markets, including MISO, SPP, and ERCOT. The evaluation relies on day-ahead solar generation forecasts, obtained from the National Renewable Energy Laboratory (NREL) [28]. The dataset contains hourly actual measurements and quantile-based forecasts for the year 2019, covering 1149 solar sites in total (751 in MISO, 172 in SPP, and 226 in ERCOT).

The first six months of observations serve as the initial calibration period and for learning cross-site correlations. Aggregated forecasts are recalibrated daily, while correlation structures are updated monthly. The most recent week of data before test day is reserved for validation and hyperparameter selection (in the case of CACP), and calibration is performed using all information available prior to the test day.

B. Baselines

The proposed method, Copula+CACP, is evaluated against the following baseline approaches:

- **NREL**: Raw fleet-level solar power forecasts provided by NREL in the form of 99 predictive quantiles. For each target coverage level, the corresponding quantiles are selected to construct prediction intervals.
- **NREL+CQR**: System-level forecasts from NREL calibrated using conformalized quantile regression (CQR).
- **NREL+CACP**: System-level forecasts from NREL calibrated using Context-Aware Conformal Prediction (CACP).
- **Copula**: Fleet-level probabilistic forecasts obtained by learning cross-site dependencies via a copula-based aggregation of site-level forecasts.

- **Copula+CQR:** Copula-based fleet-level forecasts further calibrated using conformalized quantile regression.

C. Evaluation metrics

The proposed methods are evaluated using standard performance metrics commonly adopted in probabilistic forecasting to assess both reliability and sharpness. Let $\mathcal{T}_{\text{test}}$ denote the set of time indices in the test period, with cardinality $|\mathcal{T}_{\text{test}}|$. For each time step $t \in \mathcal{T}_{\text{test}}$, let y_t denote the observed value and let $\hat{C}_t^\alpha = [\hat{C}_t^{\alpha,l}, \hat{C}_t^{\alpha,u}]$ represent the predicted $(1 - \alpha)$ prediction interval. The evaluation metrics are defined as follows:

a) *Prediction Interval Coverage Probability (PICP):* This metric measures the empirical coverage rate of the prediction intervals over the test horizon and is defined as:

$$\text{PICP}^\alpha = \frac{1}{|\mathcal{T}_{\text{test}}|} \sum_{t \in \mathcal{T}_{\text{test}}} \mathbf{1}\{y_t \in \hat{C}_t^\alpha\}. \quad (22)$$

b) *Average Interval Width (AIW):* This metric evaluates the sharpness of the prediction intervals at a specified coverage level α by averaging the interval widths across the test period:

$$\text{AIW}^\alpha = \frac{1}{|\mathcal{T}_{\text{test}}|} \sum_{t \in \mathcal{T}_{\text{test}}} \text{IW}_t^\alpha, \quad (23)$$

$$\text{IW}_t^\alpha = \hat{C}_t^{\alpha,u} - \hat{C}_t^{\alpha,l}. \quad (24)$$

c) *Winkler Score (WS):* The Winkler Score provides a combined assessment of interval sharpness and coverage by penalizing prediction intervals that fail to contain the observed value. It is computed by averaging the per-time-step scores over the test horizon:

$$\text{WS}^\alpha = \frac{1}{|\mathcal{T}_{\text{test}}|} \sum_{t \in \mathcal{T}_{\text{test}}} \text{WS}_t^\alpha, \quad (25)$$

where

$$\text{WS}_t^\alpha = \begin{cases} \text{IW}_t^\alpha + \frac{2}{\alpha}(y_t - \hat{C}_t^{\alpha,u}), & y_t > \hat{C}_t^{\alpha,u}, \\ \text{IW}_t^\alpha + \frac{2}{\alpha}(\hat{C}_t^{\alpha,l} - y_t), & y_t < \hat{C}_t^{\alpha,l}, \\ \text{IW}_t^\alpha, & \text{otherwise.} \end{cases} \quad (26)$$

All time series are normalized by the maximum generation capacity of their corresponding sites or systems to ensure comparability across different aggregation levels.

V. NUMERICAL RESULTS

A. Main Analysis

This section evaluates the performance of Copula+CACP across three large U.S. power systems: MISO, ERCOT, and SPP. The evaluation focuses on both coverage and sharpness, using evaluation metrics discussed in Section IV-C.

Table I reports the numerical results for all methods across the three ISOs at the target coverage level $1 - \alpha = 90\%$. The results indicate that the base NREL system-level forecasts are not well calibrated. For example, in MISO, the NREL forecast achieves a coverage of only 80.85%, deviating from the nominal 90% target by nearly 10 percentage points. Similar under-coverage behavior is observed for ERCOT and SPP. It is

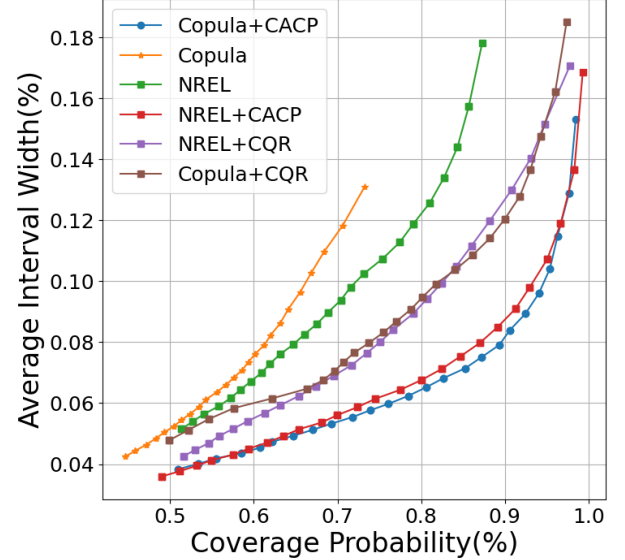


Fig. 3. Coverage–sharpness trade-off for the MISO system. The figure shows the relationship between empirical coverage and average interval width for different aggregation and calibration strategies. Copula+CACP consistently achieves lower interval widths across a wide range of coverage levels.

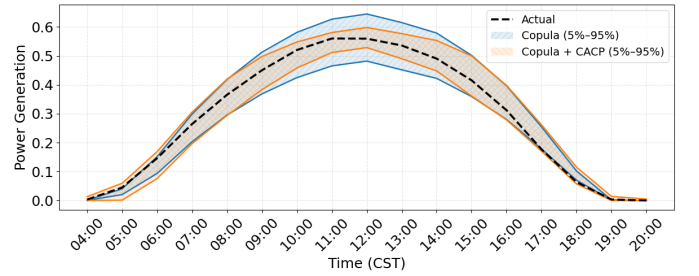


Fig. 4. Example day-ahead probabilistic forecast for the MISO system. The figure compares prediction intervals produced by Copula and Copula+CACP at the 5%–95% level. The CACP calibration step notably reduces interval width during peak generation hours while maintaining coverage.

important to note that this study assumes aggregated (system-level) probabilistic forecasts are not available in practice; NREL system-level forecasts are therefore included only as a reference baseline to demonstrate the effectiveness of the proposed framework when relying solely on site-level forecasts.

The copula-based aggregation method without calibration also exhibits poor coverage and inferior sharpness. For example, the copula method achieves only 65.51% coverage in MISO while producing wider intervals, resulting in a substantially higher WS. These results indicate that aggregation alone is insufficient to guarantee reliable probabilistic forecasts at the fleet level.

In contrast, introducing a calibration step significantly improves performance. Both CQR- and CACP-based calibration methods restore coverage closer to the target level; however, the proposed Copula+CACP method consistently achieves the best balance between coverage and sharpness. Across all three ISOs, Copula+CACP attains coverage levels close to or exceeding 90% while maintaining the narrowest prediction intervals and the lowest WSs among all competing methods.

TABLE I
PERFORMANCE COMPARISON ACROSS ISOs AT $(1-\alpha) = 90\%$

Method	MISO			ERCOT			SPP		
	PICP \uparrow	AIW \downarrow	WS \downarrow	PICP \uparrow	AIW \downarrow	WS \downarrow	PICP \uparrow	AIW \downarrow	WS \downarrow
NREL	0.8085	0.1252	0.1402	0.7501	0.1853	0.3488	0.8085	0.1363	0.1760
NREL+CQR	0.9155	0.1272	0.1395	0.8760	0.2164	0.3230	0.9081	0.1469	0.1730
NREL+CACP	0.9327	0.1011	0.1100	0.9062	0.2165	0.2826	0.9391	0.1132	0.1264
Copula	0.6551	0.0958	0.1680	0.6094	0.1301	0.4734	0.5960	0.0608	0.2522
Copula+CQR	0.8847	0.1193	0.1462	0.9039	0.2507	0.3014	0.8837	0.1235	0.1813
Copula+CACP	0.9342	0.0954	0.1066	0.9293	0.2103	0.2409	0.9172	0.0978	0.1158

The advantage of the proposed copula+CACP framework is particularly pronounced in the ERCOT system. The baseline NREL system-level forecast exhibits substantial under-coverage, achieving only 75% empirical coverage with an average interval width of 0.18. By contrast, the Copula+CACP approach increases coverage to approximately 93% with a comparable interval width of 0.21, resulting in a markedly lower Winkler Score and a more favorable calibration–sharpness trade-off. Although applying context-aware calibration directly to the NREL forecast (NREL+CACP) improves marginal coverage, the resulting prediction intervals remain wider and less sharp, as system-level calibration alone cannot fully correct for aggregation-induced dependence effects that are explicitly modeled and mitigated in the Copula+CACP framework.

Figure 3 further illustrates this behavior for MISO, showing that Copula+CACP consistently achieves lower interval widths for comparable or better coverage across a wide range of target levels. While NREL+CACP also performs strongly, the primary objective of this work is to demonstrate that comparable and in some cases slightly improved fleet-level probabilistic performance can be achieved even without access to system-level forecasts. Figure 4 further shows how the CACP step adaptively reshapes the aggregated prediction intervals on a representative day, yielding narrower intervals during peak solar generation hours when accurate uncertainty quantification is most critical.

B. Impact of Site-Level Forecasts Analysis

This section provides additional insight into the conditional coverage behavior of the proposed methods and illustrates how calibration errors at the site level influence aggregated forecasts.

Figure 5 presents the hourly conditional coverage for the MISO system at a target coverage level of 80%. In addition to system-level coverage curves, the figure overlays semi-transparent bars representing the corresponding site-level coverage at each hour. This visualization enables a direct comparison between site-level calibration quality and aggregated forecast performance over the diurnal cycle.

The results show that methods augmented with CACP consistently achieve improved conditional coverage compared to their uncalibrated counterparts. In particular, Copula+CACP and NREL+CACP remain close to the target coverage across most hours of the day, whereas the baseline Copula and

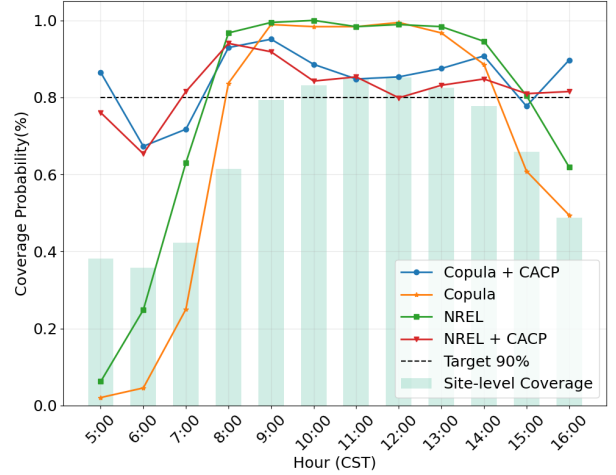


Fig. 5. Hourly conditional coverage for the MISO system at target coverage $c = 80\%$. Solid lines denote system-level coverage for different methods, while the semi-transparent bars indicate the corresponding site-level coverage.

NREL forecasts exhibit pronounced under-coverage during early morning and late afternoon periods. These deviations coincide with hours characterized by low or rapidly changing solar generation, where forecasting uncertainty is inherently higher.

The site-level coverage bars reveal substantial under-coverage during sunrise and sunset hours, which closely aligns with the degradation observed in the aggregated Copula forecast during the same periods. This alignment highlights the strong dependence of the Copula-based aggregation on the calibration quality of marginal site-level forecasts. When site-level forecasts are systematically miscalibrated, these errors propagate directly to the fleet-level aggregation, leading to conditional under-coverage.

Overall, the figure demonstrates that improving site-level calibration is critical for achieving reliable aggregated probabilistic forecasts. The effectiveness of CACP in stabilizing both site-level and system-level coverage across hours underscores its ability to mitigate the propagation of local miscalibration effects to the aggregated forecast.

VI. CONCLUSION

This paper proposed a probabilistic aggregation framework for renewable energy forecasting that combines copula-based

dependence modeling with Context-Aware Conformal Prediction (CACP). The approach is motivated by a practical industry setting in which reliable fleet-level probabilistic forecasts are required for system operations, while only lower-level probabilistic forecasts are available, and centralized fleet-level models cannot be trained due to data and scalability constraints. By explicitly modeling cross-site dependencies and applying a context-aware calibration step at the aggregated level, the framework enables the construction of reliable and sharp fleet-level forecasts directly from site-level inputs.

Empirical results on large-scale solar power systems in MISO, ERCOT, and SPP show that the proposed Copula+CACP method consistently achieves near-nominal coverage with narrower prediction intervals than existing baselines, including uncalibrated copula aggregation and direct system-level forecasts. Conditional coverage analysis further demonstrates that the proposed calibration effectively mitigates systematic miscalibration during challenging operating periods such as sunrise and sunset.

Overall, the results indicate that accurate fleet-level probabilistic forecasts can be obtained without access to raw meteorological inputs or retraining of site-level models, addressing a key limitation faced in operational practice. Future work will explore extensions to alternative dependence structures and multi-horizon forecasting.

REFERENCES

- [1] R. Teixeira, A. Cerveira, E. J. S. Pires, and J. Baptista, “Advancing renewable energy forecasting: A comprehensive review of renewable energy forecasting methods,” *Energies*, vol. 17, no. 14, p. 3480, 2024.
- [2] S. Atique, S. Noureen, V. Roy, V. Subburaj, S. Bayne, and J. Macfie, “Forecasting of total daily solar energy generation using arima: A case study,” in *2019 IEEE 9th annual computing and communication workshop and conference (CCWC)*, pp. 0114–0119, IEEE, 2019.
- [3] K. Shi, Y. Qiao, W. Zhao, Q. Wang, M. Liu, and Z. Lu, “An improved random forest model of short-term wind-power forecasting to enhance accuracy, efficiency, and robustness,” *Wind energy*, vol. 21, no. 12, pp. 1383–1394, 2018.
- [4] J. Zeng and W. Qiao, “Short-term solar power prediction using a support vector machine,” *Renewable energy*, vol. 52, pp. 118–127, 2013.
- [5] M. Xia, H. Shao, X. Ma, and C. W. De Silva, “A stacked gru-rnn-based approach for predicting renewable energy and electricity load for smart grid operation,” *IEEE Transactions on Industrial Informatics*, vol. 17, no. 10, pp. 7050–7059, 2021.
- [6] J. Jonkers, D. N. Avendano, G. Van Wallendael, and S. Van Hoecke, “A novel day-ahead regional and probabilistic wind power forecasting framework using deep cnns and conformalized regression forests,” *Applied Energy*, vol. 361, p. 122900, 2024.
- [7] C. Wan, Z. Xu, P. Pinson, Z. Y. Dong, and K. P. Wong, “Probabilistic forecasting of wind power generation using extreme learning machine,” *IEEE Transactions on Power Systems*, vol. 29, no. 3, pp. 1033–1044, 2013.
- [8] C. Sweeney, R. J. Bessa, J. Browell, and P. Pinson, “The future of forecasting for renewable energy,” *Wiley Interdisciplinary Reviews: Energy and Environment*, vol. 9, no. 2, p. e365, 2020.
- [9] Y. Zhang, J. Wang, and X. Wang, “Review on probabilistic forecasting of wind power generation,” *Renewable and Sustainable Energy Reviews*, vol. 32, pp. 255–270, 2014.
- [10] T. Hong, P. Pinson, S. Fan, H. Zareipour, A. Troccoli, and R. J. Hyndman, “Probabilistic energy forecasting: Global energy forecasting competition 2014 and beyond,” 2016.
- [11] T. Hong, P. Pinson, Y. Wang, R. Weron, D. Yang, and H. Zareipour, “Energy forecasting: A review and outlook,” *IEEE Open Access Journal of Power and Energy*, vol. 7, pp. 376–388, 2020.
- [12] Y. Wang, R. Zou, F. Liu, L. Zhang, and Q. Liu, “A review of wind speed and wind power forecasting with deep neural networks,” *Applied energy*, vol. 304, p. 117766, 2021.
- [13] A. Verdone, M. Panella, E. De Santis, and A. Rizzi, “A review of solar and wind energy forecasting: From single-site to multi-site paradigm,” *Applied Energy*, vol. 392, p. 126016, 2025.
- [14] N. E. Benti, M. D. Chaka, and A. G. Semie, “Forecasting renewable energy generation with machine learning and deep learning: Current advances and future prospects,” *Sustainability*, vol. 15, no. 9, p. 7087, 2023.
- [15] S. B. Taieb, J. W. Taylor, and R. J. Hyndman, “Coherent probabilistic forecasts for hierarchical time series,” in *International Conference on Machine Learning*, pp. 3348–3357, PMLR, 2017.
- [16] S. B. Taieb, J. W. Taylor, and R. J. Hyndman, “Hierarchical probabilistic forecasting of electricity demand with smart meter data,” *Journal of the American Statistical Association*, vol. 116, no. 533, pp. 27–43, 2021.
- [17] M. Sun, C. Feng, and J. Zhang, “Conditional aggregated probabilistic wind power forecasting based on spatio-temporal correlation,” *Applied Energy*, vol. 256, p. 113842, 2019.
- [18] A. Moradi, M. Tanneau, R. Zandehshahvar, and P. Van Hentenryck, “Enhanced renewable energy forecasting and operations through probabilistic forecast aggregation,” *arXiv preprint arXiv:2502.07010*, 2025.
- [19] H. Panamtash, Q. Zhou, T. Hong, Z. Qu, and K. O. Davis, “A copula-based bayesian method for probabilistic solar power forecasting,” *Solar Energy*, vol. 196, pp. 336–345, 2020.
- [20] H. Zhang, R. Zandehshahvar, M. Tanneau, and P. Van Hentenryck, “Weather-informed probabilistic forecasting and scenario generation in power systems,” *Applied Energy*, vol. 384, p. 125369, 2025.
- [21] V. Vovk, A. Gammerman, and G. Shafer, *Algorithmic learning in a random world*, vol. 29, Springer, 2005.
- [22] W. Wang, B. Feng, G. Huang, C. Guo, W. Liao, and Z. Chen, “Conformal asymmetric multi-quantile generative transformer for day-ahead wind power interval prediction,” *Applied Energy*, vol. 333, p. 120634, 2023.
- [23] Y. Renkema, L. Visser, and T. AlSkaif, “Enhancing the reliability of probabilistic pv power forecasts using conformal prediction,” *Solar Energy Advances*, vol. 4, p. 100059, 2024.
- [24] A. Moradi, M. Tanneau, R. Zandehshahvar, and P. V. Hentenryck, “Enhanced renewable energy forecasting using context-aware conformal prediction,” 2025.
- [25] M. Sklar, “Fonctions de répartition à n dimensions et leurs marges,” in *Annales de l’ISUP*, vol. 8, pp. 229–231, 1959.
- [26] Y. Romano, E. Patterson, and E. Candes, “Conformalized quantile regression,” *Advances in neural information processing systems*, vol. 32, 2019.
- [27] R. F. Barber, E. J. Candes, A. Ramdas, and R. J. Tibshirani, “Conformal prediction beyond exchangeability,” *The Annals of Statistics*, vol. 51, no. 2, pp. 816–845, 2023.
- [28] B. Sergi *et al.*, “ARPA-E PERFORM datasets,” 2022.

APPENDIX

Table II reports system-level probabilistic forecasting performance across ERCOT, MISO, and SPP for multiple target coverage levels. Results are shown in terms of PICP, AIW, and WS for baseline system-level forecasts and aggregation-based methods. System-level forecasts are included as reference baselines, while the aggregation results illustrate the effectiveness of the proposed Copula+CACP framework in achieving reliable and sharp fleet-level prediction intervals when only site-level forecasts are available.

TABLE II
SYSTEM-LEVEL PROBABILISTIC FORECASTING PERFORMANCE ACROSS ISOS

ISO	Method	(1- α) = 90%			(1- α) = 80%			(1- α) = 70%			(1- α) = 60%		
		PICP \uparrow	AIW \downarrow	WS \downarrow	PICP \uparrow	AIW \downarrow	WS \downarrow	PICP \uparrow	AIW \downarrow	WS \downarrow	PICP \uparrow	AIW \downarrow	WS \downarrow
ERCOT	NREL	0.7501	0.1853	0.3488	0.6910	0.1585	0.2529	0.6249	0.1350	0.2107	0.5541	0.1132	0.1826
	NREL+CQR	0.8760	0.2164	0.3230	0.7732	0.1660	0.2479	0.6864	0.1379	0.2079	0.5797	0.1123	0.1806
	NREL+CACP	0.9062	0.2165	0.2826	0.7951	0.1639	0.2240	0.6806	0.1283	0.1932	0.5584	0.1005	0.1707
	Copula	0.6094	0.1301	0.4734	0.5347	0.1017	0.3280	0.4712	0.0823	0.2628	0.4056	0.0662	0.2224
	Copula+CQR	0.9039	0.2507	0.3014	0.7938	0.1960	0.2681	0.7094	0.1486	0.2388	0.5986	0.1071	0.2121
	Copula+CACP	0.9293	0.2103	0.2409	0.8331	0.1624	0.2035	0.7264	0.1330	0.1833	0.6022	0.1093	0.1703
MISO	NREL	0.8085	0.1252	0.1402	0.7126	0.0977	0.1126	0.6423	0.0789	0.0958	0.5767	0.0641	0.0835
	NREL+CQR	0.9155	0.1272	0.1395	0.8145	0.0988	0.1123	0.7333	0.0795	0.0957	0.6578	0.0645	0.0835
	NREL+CACP	0.9327	0.1011	0.1100	0.8307	0.0745	0.0884	0.7145	0.0590	0.0775	0.6098	0.0476	0.0700
	Copula	0.6551	0.0958	0.1680	0.5989	0.0757	0.1260	0.5515	0.0633	0.1050	0.4946	0.0522	0.0906
	Copula+CQR	0.8847	0.1193	0.1462	0.7885	0.0889	0.1207	0.6902	0.0686	0.1038	0.5837	0.0539	0.0903
	Copula+CACP	0.9342	0.0954	0.1066	0.8311	0.0717	0.0872	0.7239	0.0581	0.0781	0.6060	0.0479	0.0725
SPP	NREL	0.8085	0.1363	0.1760	0.7374	0.1060	0.1380	0.6746	0.0855	0.1161	0.6043	0.0694	0.1006
	NREL+CQR	0.9081	0.1469	0.1730	0.8101	0.1079	0.1373	0.7354	0.0860	0.1156	0.6393	0.0692	0.1002
	NREL+CACP	0.9391	0.1132	0.1264	0.8441	0.0845	0.1032	0.7249	0.0674	0.0912	0.6185	0.0550	0.0838
	Copula	0.5960	0.0608	0.2522	0.5130	0.0476	0.1620	0.4637	0.0390	0.1260	0.3999	0.0319	0.1049
	Copula+CQR	0.8837	0.1235	0.1813	0.7809	0.0759	0.1434	0.6792	0.0566	0.1186	0.5812	0.0427	0.1019
	Copula+CACP	0.9172	0.0978	0.1158	0.8172	0.0755	0.0989	0.7099	0.0615	0.0895	0.6009	0.0504	0.0832